ADVANCED FUNCTIONAL MATERIALS
www.afm-journal.de

The Effect of Polymer Chain Alignment and Relaxation on Force-Induced Chemical Reactions in an Elastomer

*Brett A. Beiermann, Sharlotte L. B. Kramer, Preston A. May, Jeffrey S. Moore, Scott R. White, and Nancy R. Sottos**

Simultaneous measurements of mechanical response, optical birefringence, and fluorescence signal are acquired in situ during tensile testing of a mechanophore-linked elastomeric polymer. Mechanical stress, deformation, and polymer chain alignment are correlated with force-induced chemical reaction of the mechanophore. The mechanochemically responsive polymer under investigation is spiropyran- (SP-) linked poly(methyl acrylate) (PMA). Force-driven conversion (activation) of SP to its merocyanine (MC) form is indicated by the emergence of a fluorescence signal with 532 nm light incident on the sample. Increasing rate of tensile deformation leads to an increase in both stress and SP-to-MC conversion, indicating a positive correlation between macroscopic stress and activation. Simultaneously collected birefringence measurements reveal that rapid mechanophore activation occurs when maximum polymer chain alignment is reached. It is found that SP-to-MC conversion in PMA requires both a sufficient level of stress and adequate orientation of the polymer chains in the direction of applied force.

1. Introduction

Traditionally chemical reactions are driven by light, thermal, chemical, or electrical potential. Mechanically induced bond cleavage can also be achieved, but is typically non-selective and/or destructive.[1] By synthesizing and linking force-sensitive molecules (mechanophores) into a polymer backbone, mechanical deformation can be used to drive site-specific in situ chemical reactions. A variety of mechanophore chemistries have been incorporated into polymer backbones, and numerous force-stimulated chemical reactions have been demonstrated using pulsed sonication in the solution state.[2–12] Only a small number of mechanophores have shown activation in the solid state.[11,13,14] Notably, Davis et al. achieved force-induced activation of spiropyran (SP), which undergoes a 6-π electro-cyclic ring-opening reaction under tensile deformation to a merocyanine (MC) form.

The reaction of SP to MC is indicated by a strong color change, due to absorbance in the visible range, as well as the emergence of a fluorescence signal.[13,15,16] This mechanically induced color change could serve as a sensor for mechanical deformation or stress in a polymer sample. Mechanochromic functionality has been demonstrated in previous polymer systems,[17,18] but the mechanophore approach is unique in that covalent bonds are cleaved by force and chemical rearrangement of the mechanophore occurs.

Understanding the parameters influencing transfer of macroscopic stress in a bulk polymer to localized force on the mechanophore remains a topic of active research. The mechanophore, SP, has been incorporated into a variety of solid state polymers[15,16,19,20] and the ease of monitoring the SP to MC conversion makes this system ideal for studying many of the key parameters affecting mechanophore activation in bulk polymers. However, the effects of applied stress, deformation and polymer chain orientation have not yet been fully explored. Previous publications have alluded to the importance of polymer orientation and alignment in the direction of applied force for achieving mechanochemical reactions.[19,20] Recent work by Beiermann et al.[21] examined the orientation of the mechanophore subunits within the polymer backbone using polarized fluorescence and found a preferential activation of mechanophores in the direction of macroscopic force. However, the orientation of polymer chains during loading and the influence on mechanophore activation have not yet been quantitatively correlated.

The proposed premise for mechanophore activation in bulk polymers is that linearly oriented polymer chains, aligned in the direction of macroscopic stress, transfer force to the mechanophore more efficiently than randomly oriented chains, which will first use the mechanical energy to align the chain in the direction of force. To investigate this hypothesis, we simultaneously measured stress, stretch ratio, mechanophore fluorescence, (a measure of SP activation to MC) and

Dr. B. A. Beiermann, Dr. S. L. B. Kramer, P. A. May, J. S. Moore, Prof. S. R. White, Prof. N. Sottos
405 N. Matthews Avenue
Urbana, IL, 61801, USA
E-mail: n-sottos@illinois.edu
Dr. B. A. Beiermann, Prof. N. R. Sottos
Department of Materials Science and Engineering
University of Illinois at Urbana-Champaign
Urbana, IL 61801, USA
Dr. P. A. May, Prof. J. S. Moore
Department of Chemistry
University of Illinois at Urbana-Champaign
Urbana, IL 61801, USA
Prof. S. R. White
Department of Aerospace Engineering
University of Illinois at Urbana-Champaign
IL 61801, USA

DOI: 10.1002/adfm.201302341

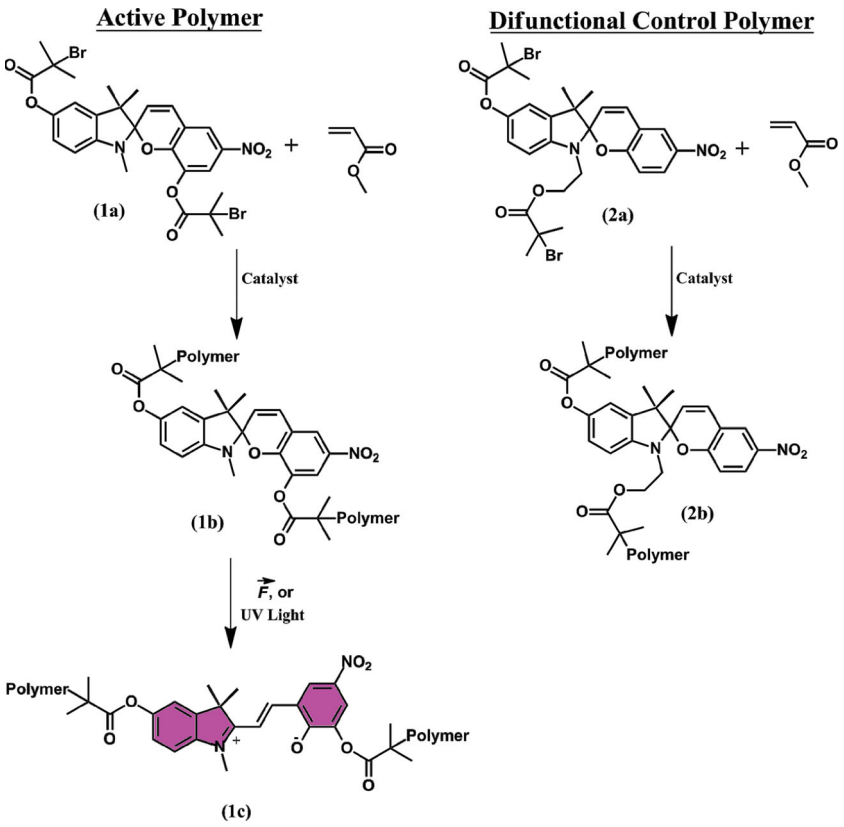

Scheme 1. Synthesis of vinyl polymers from α-bromo ester functionalized SP initiators. 1a) Active SP, 1b) active SP-linked polymer, and 1c) ring-opened (activated) MC form. 2a) Difunctional control SP, and 2b) difunctional control SP-linked polymer.

optical birefringence (a relative measure of polymer chain orientation).[22]

The mechanical and optical response of the polymer and mechanophore were monitored for a range of tensile stretch rates, as well as under stress relaxation conditions. SP activation was correlated with mechanical behavior and polymer chain alignment from simultaneously obtained in situ birefringence measurements, providing insight for achieving force-induced activation in solid state mechanophore-linked polymer systems.

2. Results and Discussion

2.1. Materials and Synthesis

Linear mechanochemically active SP-linked PMA was synthesized using SP as a living radical initiator as described by Davis et al.[13] By this method SP was covalently bonded into roughly the center of a polymer chain. Control PMA was also synthesized with SP linked into the backbone such that force was not transferred across the sensitive C–O spiro bond. This linkage is referred to throughout this manuscript as difunctional control SP-linked PMA. Active and difunctional control SP chemical structures are included in the **Scheme 1**.

Polymers were synthesized with number average molecular weights of ≈180 kDa, and polydispersity below 1.2. Glass transition temperatures (T_g) for active and control polymer were 12 °C and 13 °C, respectively, taken as the shoulder of differential scanning calorimetry curves. These values agreed closely with plain PMA (no SP). The effect of SP incorporation on polymer thermo-mechanical properties was considered negligible.

2.2. Simultaneous Measurement of Stress, Fluorescence, and Birefringence

Measurements for load, displacement, birefringence and fluorescence intensity were captured simultaneously during monotonic tensile testing using a novel optical and mechanical setup. A schematic and photo of the setup are shown in **Figure 1**a,b, respectively. A circularly polarized incident light source was incident on a polymer sample, which acted both as a monochromatic light source for photoelasticity (birefringence measurement) and an excitation source for fluorescence of the activated MC form (Species 1c in Scheme 1) of the mechanophore.

The incident wavelength (Λ_{light} = 532 nm) was reflected off a dichroic beamsplitter at 45° incidence after passing through the sample for the photoelastic beam, while higher wavelengths (Λ_{light} > 580 nm) were transmitted through the dichroic beamsplitter for collection of the fluorescence signal. The photoelastic beam was then separated into four identical beams (I_1–I_4, see Supporting Information for thorough description) using a two-dimensional diffraction grating, and the resulting images were passed through polarization optics such that the photoelastic state could be fully characterized. The birefringence signal was then calculated by a phase stepping procedure reported by Kramer et al.[23] By this method, full-field fluorescence and birefringence signals were simultaneously captured during tensile testing of dog-bone shaped specimens. Representative images for data collection are provided in **Figure 2**a–d, along with an optical image of a sample before and after tensile testing (Figure 2e). The experimental method is more thoroughly described in the Experimental Section.

Stretch ratio (λ, defined as instantaneous sample gauge length divided by the un-deformed gauge length) and true stress (σ_{true}, calculated based on optically measured sample width, and assuming the width and thickness stretch ratios were equivalent) were determined from the applied displacement and measured load. Representative data for a mechanochemically active sample tested at a stretch rate ($d\lambda/dt$) of 0.02 s^{-1} are plotted in **Figure 3**. Stress increased consistently as a function of increasing stretch ratio until failure, which typically occurred at a stretch ratio between 10 and 12. An increase in slope of the stress versus stretch ratio plot ($d\sigma/d\lambda$), that is, hardening, occurred with increasing deformation. Birefringence (Δn) had

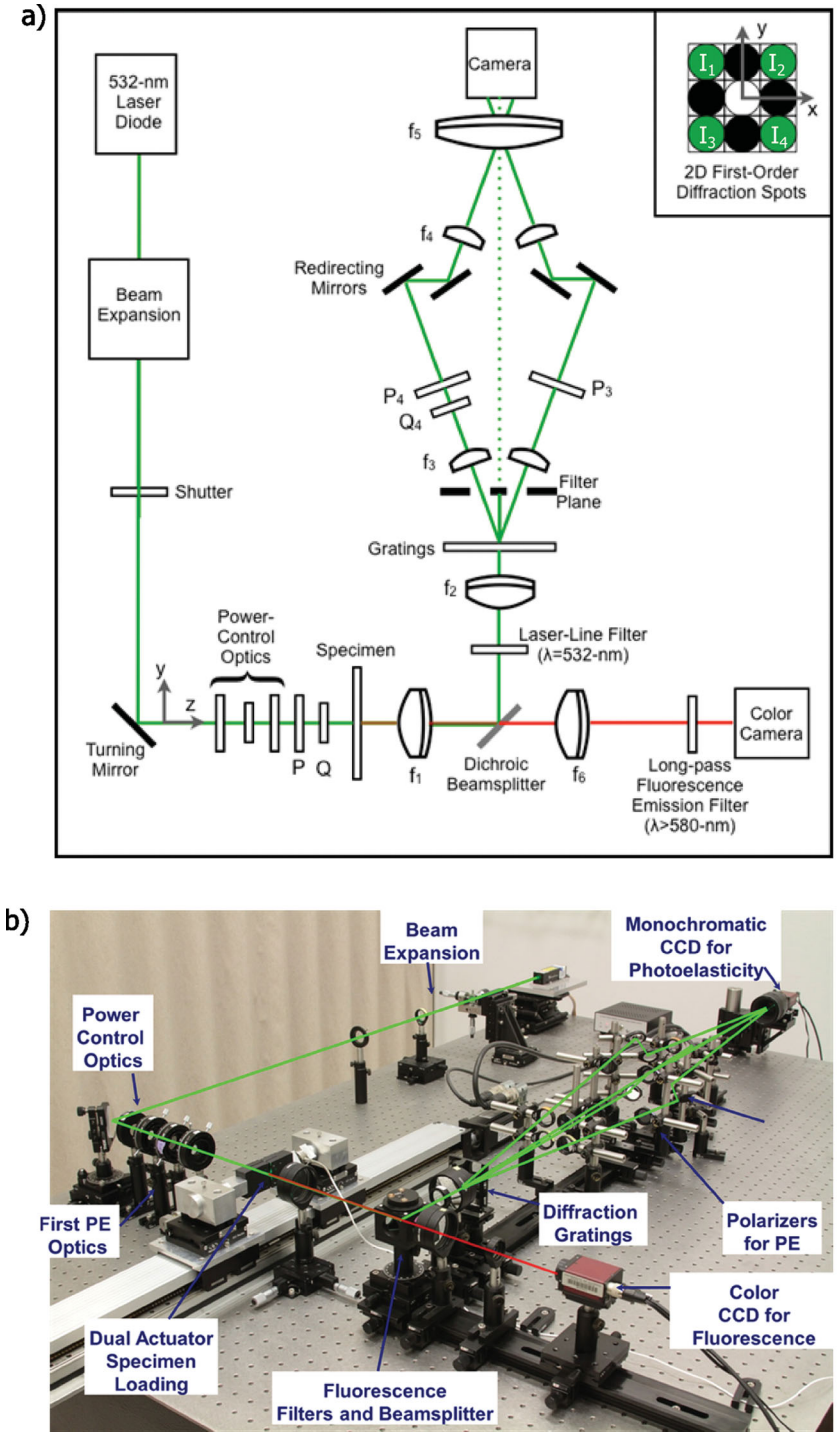

Figure 1. Design of optical setup. a) Over-head view schematic showing two of the four photoelastic (PE) beams (I_1 and I_2). I_3 and I_4 are mirrored across the x–z plane. Optical elements are indicated by P – linear polarizer, Q – quarter wave plate, and f – focusing lens. b) Photo with incident (green) and fluorescent light (red) illustrated. A monochromatic laser was used for both photoelasticity measurements and excitation of fluorescence. The photoelastic and fluorescence signals were separated with a dichroic beam splitter. The fluorescence light was imaged using a color camera. The photoelastic light was split using 2D diffraction, and the (±1,±1) beams, shown as the four green first-order diffraction spots in the inset in (a), were passed through appropriate polarization optics for I_1–I_4 and redirected to a single camera.

a negative value with respect to the tensile direction, agreeing with previously published data by Saiz et al.,[24] an effect likely due to bulky pendant methacrylate groups on the PMA backbone. In Figure 3 the birefringence value is plotted as the magnitude (Δn multiplied by -10^3), which increased with increasing stretch ratio, indicating alignment of the polymer backbone in the direction of loading, and then leveled out as the polymer chains reached maximum alignment. The intensity of the measured fluorescence signal ($I_{fl,raw}$) was assumed proportional to the amount of reacted SP, that is, MC, in the beam path.[15] At room temperature (RT = 22 °C), a small equilibrium amount of MC was present in all specimens, which led to some fluorescence signal prior to stretching ($\lambda = 1$). During the initial loading, the fluorescence signal decreased due to sample thinning (i.e., a lower concentration of mechanophores in the fluorescence image field of view). With increasing stretch ratio, the fluorescence intensity began to increase, indicating mechanical activation of SP to the fluorescent MC form. The onset of detectable activation was defined where the increase in activation was significant enough to counteract the effect of thinning. Thus the activation stretch, λ^*, was identified as the lowest stretch ratio with a positive slope of raw fluorescence intensity, $I_{fl,raw}$ versus stretch ratio, λ, as indicated in Figure 3.

2.3. Effect of Stretch Rate

2.3.1. Stretch Rate Variation in Active SP-Linked PMA

Active PMA samples were tested at stretch rates of 0.004 s^{-1}, 0.02 s^{-1}, and 0.10 s^{-1}. The resulting polymer behavior (stress, birefringence, and fluorescence intensity) are plotted in **Figure 4** for representative samples at each stretch rate. The stress (Figure 4a) in the polymer samples increased with increasing stretch rate as expected for an elastomeric material. In virtually all samples, hardening was observed with increasing stretch ratio. Birefringence (Figure 4b) also increased with increasing stretch rate. Birefringence values began to plateau for all stretch rates as the chains became maximally aligned in the direction of force. The fluorescence signal, $I_{fl,raw}$, was adjusted for the number of mechanophores in the field of view and normalized by the fluorescence intensity at ambient equilibrium ($\lambda = 1$) fluorescence intensity, as described in the Experimental Section.

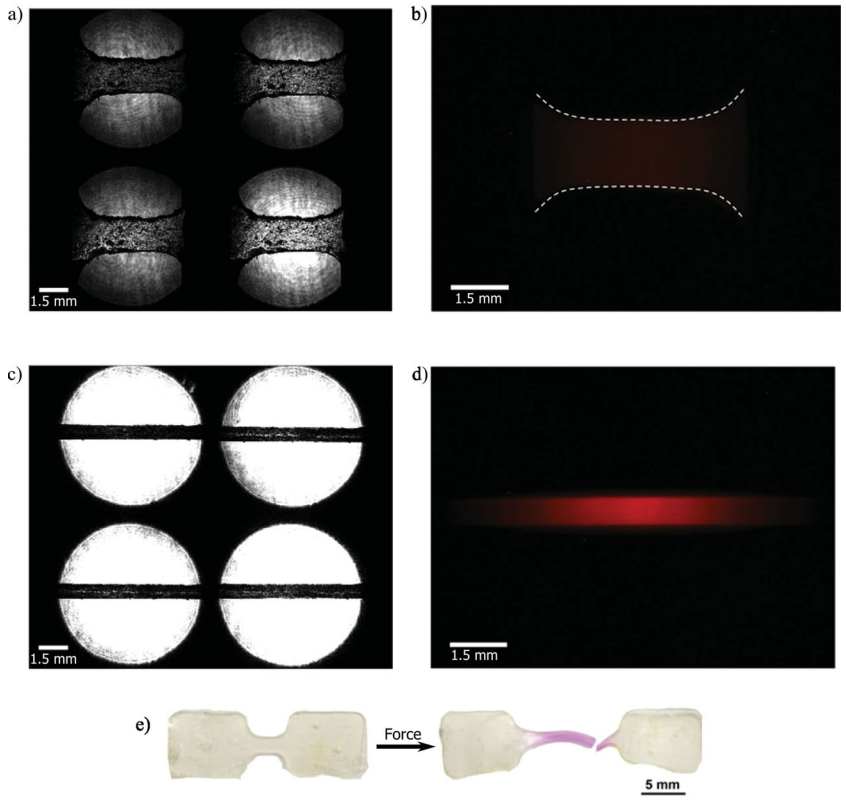

Figure 2. Optical data collection for simultaneously obtained birefringence and fluorescence measurement. a) Four photoelastic patterns (I_1 upper left; I_2 upper right; I_3 lower left; and I_4 lower right) for $\lambda = 1.0$; b) fluorescence image for $\lambda = 1.0$ with the edges of the sample outlined in dashed white lines; c) four photoelastic patterns for $\lambda = 9.0$; and d) fluorescence image for $\lambda = 9.0$. e) Representative image of a polymer sample before and after tensile testing to failure.

Representative normalized fluorescence, $I_{fl,norm}$, can be found in Figure 4c. For all stretch rates, rapid activation of SP (increase in $I_{fl,norm}$) at large stretch ratios coincided with a plateau in the birefringence, during which polymer chains approached maximum alignment and hardening occurred. Increased birefringence and activation were considerably more apparent in the fastest testing rate (0.10 s^{-1}) when compared with middle and slowest stretch rates (0.004 s^{-1} and 0.02 s^{-1}). This finding implies that larger macroscopic stress at higher stretch rate leads to greater chain alignment and force across the mechanophore, causing more extensive activation of SP.

Figures 5a–c reveal the trend in stretch ratio, stress, and birefringence, at the activation point, as defined in Section 2.2, averaged over three samples at each stretch rate. The stretch value at activation, λ^* shows a marked decrease at the fastest stretch rate. The true stress at the activation point, σ^* shows an increasing trend, indicating that although macroscopic stress is positively correlated to SP activation, the same macroscopic stress does not necessarily translate to the same force and activation of SP at the molecular scale. This effect is attributed to rate dependent hardening of the bulk polymer (Figure 4a), which leads to viscoelastic redistribution of intermolecular forces, i.e. chain slip and relaxation. Activation birefringence, Δn^*, values were similar between stretch rates, indicating that a similar degree of chain alignment was present at the onset of SP activation, regardless of the stretch rate. Finally, the rate of change of fluorescence intensity with respect to stretch ratio ($dI_{fl,norm}/d\lambda$) was averaged between stretch ratios of 8 and 9, where all samples showed an increasing fluorescence signal, but none had failed. The results plotted in Figure 5d show a clear trend of higher rate of fluorescence change (i.e., SP activation) with increasing stretch rates.

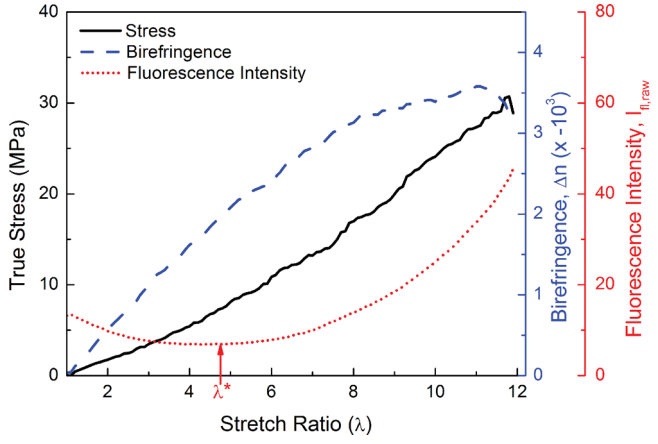

Figure 3. Simultaneously obtained stress, birefringence and raw fluorescence intensity as a function of stretch ratio at a stretch rate of 0.02 s^{-1}. The activation point at λ^* is indicated.

2.3.2. Stretch Rate Variation in Difunctional Control SP-Linked PMA

Difunctional control SP-linked PMA was tested in tension at the same stretch rates as mechanochemically active polymer. Stress, birefringence and normalized fluorescence data are shown in **Figure 6**. The mechanical and birefringence behavior were similar to the mechanochemically active case. Despite being linked in a manner that should not transmit force from the covalently bonded polymer chains across the mechanophore, an increase in fluorescence signal (activation) was seen with increasing stretch ratio. The extent of fluorescence increase was lower than the active case, but still showed stretch rate dependence (higher stretch rate led to greater activation). In contrast to active specimens, color change was not visually detectable in the gauge section of difunctional control SP-linked samples after tensile testing (see Figure S2 in the Supporting Information).

The fluorescence increase in difunctional control PMA had a virtually identical spectroscopic fluorescence peak as the active sample (refer to Figure S1 in the Supporting Information),

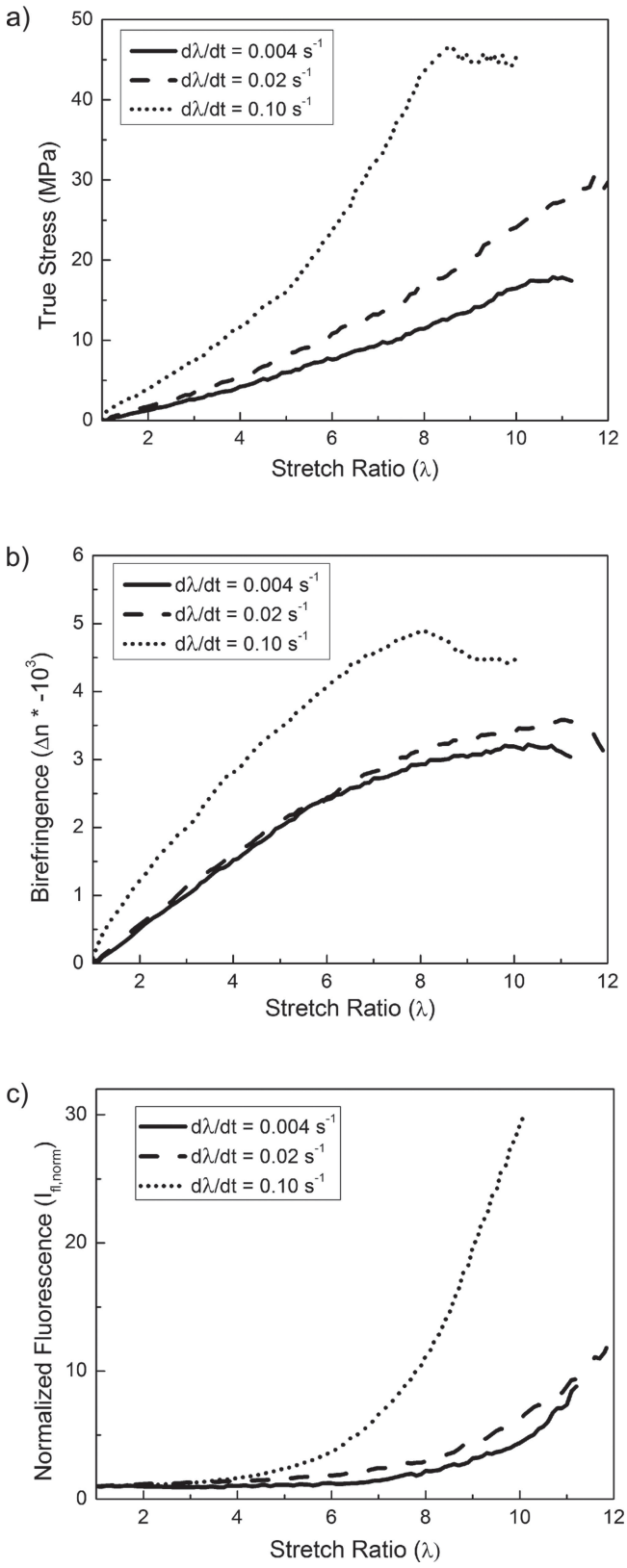

Figure 4. Representative properties of active SP-linked PMA at stretch rates ($d\lambda/dt$) of 0.004 s^{-1}, 0.02 s^{-1}, and 0.10 s^{-1}. a) True stress versus stretch ratio, b) birefringence versus stretch ratio, and c) thickness-corrected, normalized fluorescence intensity versus stretch ratio.

and no fluorescence signal was present in polymer without SP incorporated, providing evidence that fluorescence increase in the difunctional control was due to SP ring opening. Fluorescence increase in the difunctional control SP-linked PMA may be due to a frictional force on the pendant group containing the force sensitive C–O spiro bond (Scheme 1, Species 2). This effect is discussed in more detail in Section 2.4.2.

2.4. Stress Relaxation Behavior of SP-Linked PMA

2.4.1. Active SP-linked PMA

Active SP-linked PMA samples were drawn at a stretch rate of 0.10 s^{-1} to a stretch ratio of 9 and held at constant deformation. The relaxation response of stress, birefringence and activation were measured as a function of time and are shown in **Figure 7**. The stress and birefringence during the stress relaxation stage were fit to exponential decay curves with effective time constants (τ_{eff}) of 54 s and 83 s, respectively (Figure S3 in Supporting Information).

During stress relaxation, the fluorescence intensity in the polymer continued to increase, indicating a time dependence of force-induced chemical reactions. Although macroscopic deformation had stopped, stress in the system was sufficient to drive the reaction forward without further deformation. The fluorescence reached a maximum as the stress decayed and eventually decreased slightly over time due to the incident light source (Λ = 532 nm) driving MC to SP. SP to MC activation continued to proceed forward until the stress in the sample was below ≈10 MPa. This relaxation behavior was repeatable over multiple samples. The stress relaxation region of Figure 7 in which normalized fluorescence intensity increased was fit to an exponential curve. The effective time constant of the fluorescence increase was 53 s, virtually the same as the stress relaxation time constant. After returning to zero load, some fluorescence increase remained in the sample.

Effective time constants measured from stress and birefringence relaxation conditions (fitted to exponential decay for 400 s after the onset of relaxation) were between 50–100 s at all loading rates. These relaxation time scales were similar to the test time for the fastest stretch rate ($d\lambda/dt$ = 0.10 s^{-1}). Slower stretch rates ($d\lambda/dt$ = 0.004 s^{-1} and $d\lambda/dt$ = 0.02 s^{-1}) corresponded to test times substantially longer than the relaxation times ($t_{test} \approx 5–25\ \tau_{eff}$), giving more time for polymer relaxation. The pronounced increase in stress, birefringence, and activation at the highest stretch rate of 0.10 s^{-1} (refer to Figure 4) is attributed to a less prominent relaxation effect over short test durations.

2.4.2. Difunctional Control SP-linked PMA

Difunctional control SP-linked PMA specimens were subjected to stress relaxation testing similar to the active case. The response of the difunctional control polymer over time is included in **Figure 8**. The fluorescence signal increased during deformation, implying activation of SP to MC. In contrast to the active samples, the fluorescence signal did not continue to increase in the stress relaxation stage. Instead the fluorescence

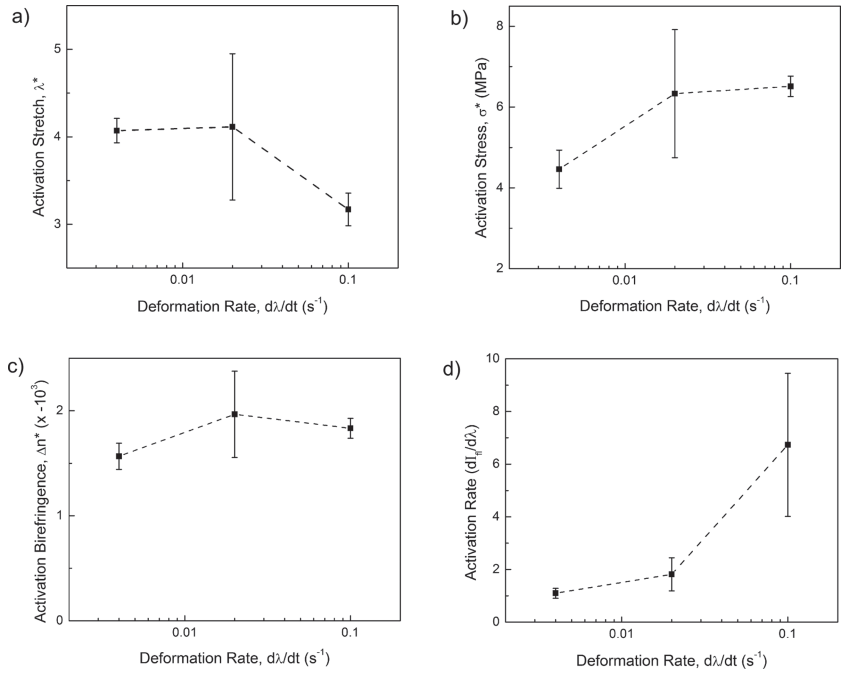

Figure 5. Activation points for SP-linked PMA as a function of stretch rate. a) Activation stretch, λ^*, b) activation stress, σ^*, c) activation birefringence, Δn^* and d) average activation rate ($dI_{fl,norm}/d\lambda$) between $\lambda = 8$ and $\lambda = 9$.

signal decreased slightly during relaxation indicating that on average SP to MC conversion had stopped proceeding forward, and was slowly reverted by the incident light source.

The stress relaxation response indicated a differing mechanism for fluorescence increase (i.e., activation) of difunctional control SP-linked PMA when compared to active polymer. Activation of control SP during stretching may be due to a drag force in the polymer and mechanophore from solvent friction. Polymer dynamics theory, based on Rouse[25] and Zimm[26] models, assumes that solvent friction, ξ, applies drag force on a flowing polymer chain.[27,28] Polymer drag force is the product of a drag coefficient from polymer interaction with solvent (in this case other polymer chains), and the rate of polymer flow. The experimental data exhibited the expected trends for drag force-induced activation of the control SP, with activation (fluorescence increase) increasing with increasing stretch rate (polymer flow), and no activation during stress relaxation when the rate of polymer flow (therefore drag force) was negligibly small.

3. Conclusions

SP-linked PMA provided a model system for measuring the mechanochemical response in an elastomeric polymer. Previous work by Davis et al.[13] demonstrated mechanophore activation when linked into a PMA backbone under tensile deformation via a color change. The work presented in this manuscript provides a thorough mechanical and optical study of a SP-linked PMA subjected to a tensile load to determine the parameters which affect mechanophore activation in an elastomeric polymer.

A novel experimental set-up was designed to simultaneously apply a mechanical load to polymer samples and collect in situ optical measurements of fluorescence and polymer chain alignment. The SP-to-MC conversion was monitored via the fluorescence signal of the MC form, excited by a 532 nm laser and collected at $\Lambda > 580$ nm. Birefringence provided a relative measure of the polymer chain alignment, which was correlated to the mechanophore activation. The findings indicate that rapid activation of SP occurred when birefringence began to plateau and reach a maximum, thus when polymer chains were most aligned in the direction of macroscopic force.

The effect of tensile stretch rate was studied and showed that for increasing stretch rate, the macroscopic stress in the polymer increased and a corresponding increase in the rate and degree of activation ensued. Stress relaxation behavior of SP-linked PMA indicated that SP activation is a time dependent process, and mechanochemical conversion will continue at a constant deformation, provided that the stress remains sufficiently high (above ≈10 MPa).

An SP-linked control was incorporated into the PMA backbone such that force was not transferred across the sensitive C–O spiro bond of the mechanophore. In this configuration, some amount of fluorescence increase, that is, SP activation, was detected in the control under tension. The fluorescence increase was of smaller magnitude and did not continue under stress relaxation conditions, indicating a different mechanism for activation in the control case.

4. Experimental Section

Sample Preparation: Active and difunctional control SP-linked PMA were synthesized via single electron transfer living radical polymerization reactions with SP serving as the initiator as described by Davis et al.[13] Polymer was dissolved into THF, filtered through fumed silica and dried under vacuum at 50 °C for 24 h. This step was critical to removing all solvents involved in synthesis and attaining maximum polymer stiffness. PMA was then molded at a pressure of 200 psi at 150 °F (66 °C) for 10 min in a closed mold.

Tensile Testing Protocol: For monotonic tensile testing, displacement control was used at stretch rate was 0.1 s^{-1}, 0.02 s^{-1}, and 0.004 s^{-1}. Images were acquired at periods of 1 s, 5s, and 25 s for the three testing rates, respectively. For the stress relaxation testing, samples were stretched to approximately $\lambda = 9$, held at constant displacement. The image acquisition rates were the same as the monotonic tests. True stress was calculated during testing based on the load, F, in the sample and the optically measured sample width, w, based on photoelastic image. The thickness (T) stretch ratio, $\lambda^T = T/T_0$, was assumed equal to the optically measured width stretch ratio, $\lambda^w = w/w_0$, therefore true stress was defined as

$$\sigma_{true} = \frac{F}{w_0 T_0 (\lambda^w)^2} \quad (1)$$

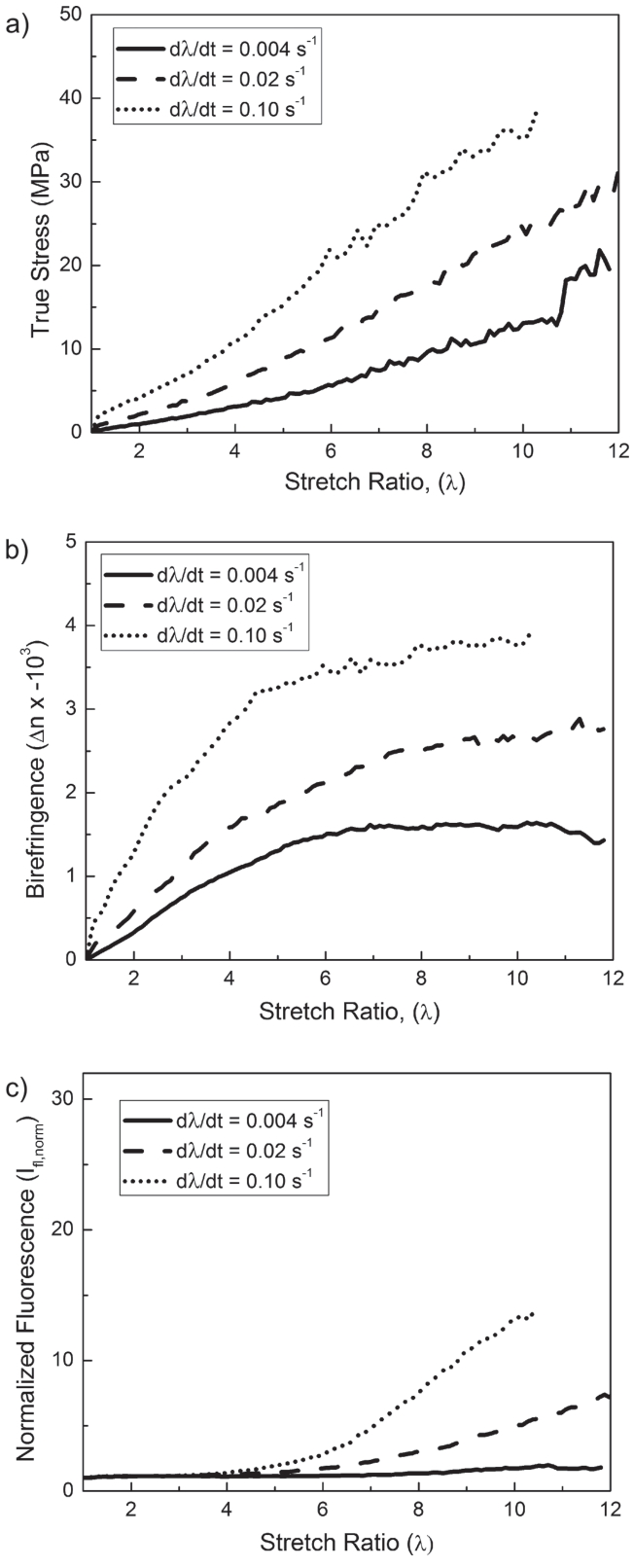

Figure 6. Behavior of difunctional control SP-linked PMA loaded in tension at three stretch rates. a) Stress vs stretch ratio, and b) birefringence vs stretch ratio, and c) thickness-corrected, normalized fluorescence intensity vs stretch ratio.

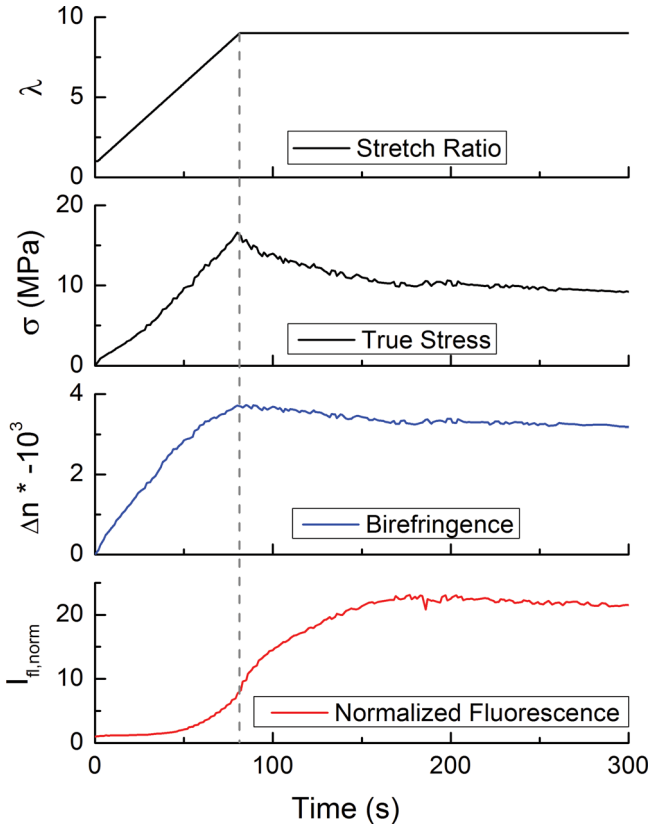

Figure 7. Stress relaxation testing of active SP-linked PMA loaded at a stretch rate of 0.10 s^{-1} including stretch history, stress relaxation, birefringence relaxation, and normalized fluorescence intensity as a function of time.

Combined Mechanical and Optical Experimental Setup: The experimental setup, shown in Figure 1, incorporated a uniaxial load frame with a hybrid optical measurement technique combining fluorescence imaging and photoelasticity. This setup allowed for simultaneous measurement of load-displacement data, fluorescence detection (indicating SP activation to MC), and optical birefringence (a relative measure of polymer chain orientation) using a photoelastic polariscope. A custom uniaxial load fame from IMAC Motion Control Corporation utilized two opposing actuators so that the center of a tensile sample remained in the field of view. A 5-lb (22 N) capacity Honeywell Sensotec Load Cell (Model 31) was attached to one of the actuators to monitor load. Displacement of the actuators was controlled through NI LabVIEW. The load frame was oriented horizontally on an optical table to allow for the hybrid optical techniques.

A 532-nm laser diode was the source for both photoelasticity and florescence imaging excitation. The laser beam was expanded to a 12-mm diameter collimated beam, passing though polarization optics to control the light intensity and to create a circularly polarized beam for the first portion of the photoelastic polariscope. After the light was transmitted through the sample, a dichroic beamsplitter from Chroma Technologies reflected the incident light wavelength (Λ = 532) for photoelastic imaging and transmitted emitted fluorescence from the MC form, which has a broad emission peak centered at 600–650 nm when excited with 532 nm light (see Supporting Information for spectra). To determine the optical birefringence from the photoelastic signal, we utilized phase-stepped photoelasticity requiring four different images obtained from four different combinations of analyzing polarization optics after the sample, typically obtained by rotating these optics for sequential image capture.[29,30] Since PMA is a time-dependent

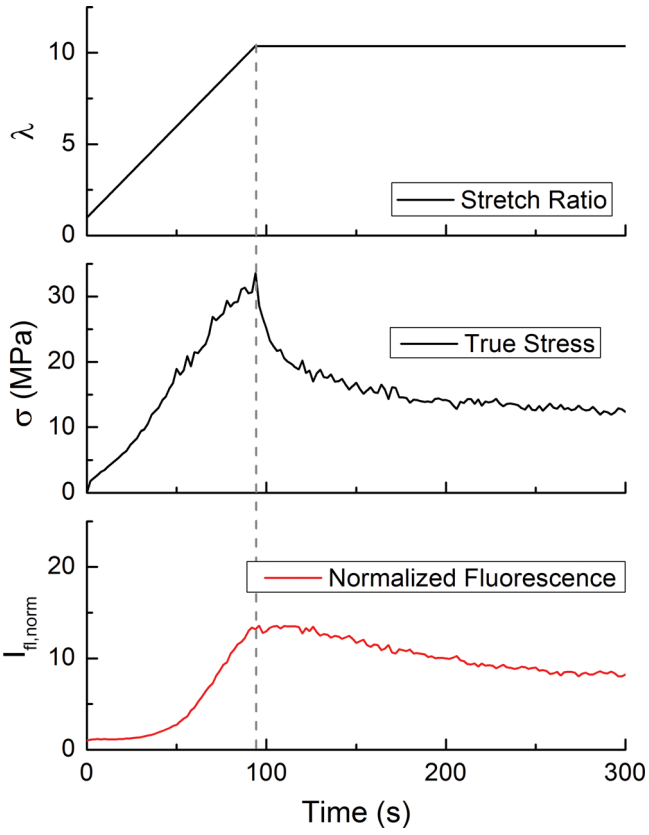

Figure 8. Stress relaxation and activation in difunctional control SP-linked PMA loaded at a stretch rate of 0.10 s^{-1}.

viscoelastic material, it did not allow sequential phase-stepping photoelastic images. Therefore diffraction gratings were used to split the photoelastic signal into four beams that were captured by the same camera (AVT Stingray F145b), allowing for four simultaneous phase-stepped images.[23] A mathematical description of the birefringence calculation is included in the SI. The fluorescent signal from MC was further filtered by a long-pass emission filter for wavelengths greater than 580-nm from Chroma Technologies, and the image was recorded on a color camera (AVT Stingray F504c). Figure 2 shows representative images of the four simultaneously captured phase-stepped photoelastic images from one camera and of the fluorescence image from the other camera for a SP-linked PMA tensile sample before ($\lambda = 1$) and during tensile testing ($\lambda = 9$).

Constant fluorescence imaging conditions (180 μW laser power, 800 ms exposure) were maintained for all tests. At this laser power conversion of MC to SP was relatively insignificant, and a mechanical shutter between the laser and sample blocked the laser between fluorescence images to minimize loss of the fluorescence signal.

Image Analysis for Fluorescence and Birefringence Measurement: Fluorescence and birefringence images were analyzed in order to obtain relative quantities for activation and chain alignment. A relative measure of fluorescence intensity, $I_{fl,raw}$, was calculated using the red channel intensity of the color image, averaged over pixels in the gauge section of the sample. Pixels within ≈10 pixels of the sample edge were not included to minimize fluorescence edge effects. As described in detail in the Supporting Information, the normalized fluorescence, $I_{fl,norm}$, was obtained by correcting for the change in the number of SP in the field of view of the camera due to the large thickness change during the course of each test, and normalizing to the equilibrium fluorescence intensity ($I_{fl,raw,0}$) of the sample, that is, $I_{fl,raw}$ at $\lambda = 1$. Additionally, the corrected fluorescence signal was averaged over all pixels within the gage section of the field of view. The equation relating the normalized fluorescence to the raw fluorescence, measured length stretch ratio, λ, and width stretch ratio, λ^w is

$$I_{fl,norm} = \frac{I_{fl,raw}\lambda\lambda^w}{I_{fl,raw,0}} \quad (2)$$

This calculation is derived in the Supporting Information.

The optical birefringence of the polymer was determined from the four phase-stepped photoelastic images, as described in detail in the Supporting Information. In summary, the intensities of the four interference patterns were averaged over the same central area of interest in the gauge section of the sample, and then used to calculate the isochromatic phase, δ, which is a measure of the relative retardation of the polarized light through the sample. The isochromatic phase is directly related to the optical birefringence, Δn, by

$$\delta = \Delta n \frac{2\pi T}{\Lambda} \quad (3)$$

where T is the current thickness (as determined from the width stretch ratio) and Λ is the wavelength of the incident light.

Supporting Information

Supporting Information is available from Wiley Online Library or from the author.

Acknowledgements

B.A.B. and S.L.B.K. contributed equally to this work. This work was supported by a MURI grant from the Army Research Office, grant number W911NF-07–1–0409. The authors thank the Beckman Institute for Science and Advanced Technology and the Aerospace Engineering machine shop at the University of Illinois for their assistance in this work.

Received: July 12, 2013
Revised: September 9, 2013
Published online: November 8, 2013

[1] M. K. Beyer, H. Clausen-Schaumann, *Chem. Rev.* **2005**, *105*, 2921.
[2] S. L. Potisek, D. A. Davis, N. R. Sottos, S. R. White, J. S. Moore, *J. Am. Chem. Soc.* **2007**, *129*, 13808.
[3] C. R. Hickenboth, J. S. Moore, S. R. White, N. R. Sottos, J. Baudry, S. R. Wilson, *Nature* **2007**, *446*, 423.
[4] J. M. Lenhardt, A. L. Black, S. L. Craig, *J. Am. Chem. Soc.* **2009**, *131*, 10818.
[5] A. G. Tennyson, K. M. Wiggins, C. W. Bielawski, *J. Am. Chem. Soc.* **2010**, *132*, 16631.
[6] J. M. J. Paulusse, R. P. Sijbesma, *Chem. Commun.* **2008**, 4416.
[7] A. Piermattei, S. Karthikeyan, R. P. Sijbesma, *Nat. Chem.* **2009**, *1*, 133.
[8] M. J. Kryger, M. T. Ong, S. A. Odom, N. R. Sottos, S. R. White, T. J. Martinez, J. S. Moore, *J. Am. Chem. Soc.* **2010**, *132*, 4558.
[9] A. L. Black, J. M. Lenhardt, S. L. Craig, *J. Mater. Chem.* **2011**, *21*, 1655.
[10] Z. Huang, R. Boulatov, *Chem. Soc. Rev.* **2011**, *40*, 2359.
[11] A. L. B. Ramirez, Z. S. Kean, J. A. Orlicki, M. Champhekar, S. M. Elsakr, W. E. Krause, S. L. Craig, *Nat. Chem.* **2013**, *5*, 757.
[12] H. M. Klukovich, T. B. Kouznetsova, Z. S. Kean, J. M. Lenhardt, S. L. Craig, *Nat. Chem.* **2013**, *5*, 110.

[13] D. A. Davis, A. Hamilton, J. L. Yang, L. D. Cremar, D. Van Gough, S. L. Potisek, M. T. Ong, P. V. Braun, T. J. Martinez, S. R. White, J. S. Moore, N. R. Sottos, *Nature* **2009**, *459*, 68.
[14] J. M. Lenhardt, A. L. Black, B. A. Beiermann, B. D. Steinberg, F. Rahman, T. Samborski, J. Elsakr, J. S. Moore, N. R. Sottos, S. L. Craig, *J. Mater. Chem.* **2011**, *21*, 8454.
[15] B. A. Beiermann, D. A. Davis, S. L. B. Kramer, J. S. Moore, N. R. Sottos, S. R. White, *J. Mater. Chem.* **2011**, *21*, 8443.
[16] C. M. Kingsbury, P. A. May, D. A. Davis, S. R. White, J. S. Moore, N. R. Sottos, *J. Mater. Chem.* **2011**, *21*, 8381.
[17] R. A. Nallicheri, M. F. Rubner, *Macromolecules* **1991**, *24*, 517.
[18] B. R. Crenshaw, M. Burnworth, D. Khariwala, A. Hiltner, P. T. Mather, R. Simha, C. Weder, *Macromolecules* **2007**, *40*, 2400.
[19] C. K. Lee, D. A. Davis, S. R. White, J. S. Moore, N. R. Sottos, P. V. Braun, *J. Am. Chem. Soc.* **2010**, *132*, 16107.
[20] G. O'Bryan, B. M. Wong, J. R. McElhanon, *ACS Appl. Mater. Interfaces* **2010**, *2*, 1594.
[21] B. A. Beiermann, S. L. B. Kramer, J. S. Moore, S. R. White, N. R. Sottos, *ACS Macro Lett.* **2011**, *1*, 163.
[22] E. M. Arruda, P. A. Przybylo, *Polym. Eng. Sci.* **1995**, *35*, 395.
[23] S. Kramer, B. Beiermann, S. White, N. Sottos, *Exp. Mech.* **2013**, 327.
[24] E. Saiz, E. Riande, J. E. Mark, *Macromolecules* **1984**, *17*, 899.
[25] J. P. E. Rouse, *J. Chem. Phys.* **1953**, *21*, 1272.
[26] B. H. Zimm, *J. Chem. Phys.* **1956**, *24*, 269.
[27] A. Soranno, B. Buchli, D. Nettels, R. R. Cheng, S. Müller-Späth, S. H. Pfeil, A. Hoffmann, E. A. Lipman, D. E. Makarov, B. Schuler, *Proc. Natl. Acad. Sci.* **2012**, *109*, 17800.
[28] S. J. Hagen, *Curr. Protein Peptide Sci.* **2010**, *11*, 385.
[29] S. Barone, G. Burriesci, G. Petrucci, *Exp. Mech.* **2002**, *42*, 132.
[30] E. A. Patterson, Z. F. Wang, *J Strain Anal. Eng. Design* **1998**, *33*, 1.